Supporting Information

A New Type of BiPO$_4$ Oxy-acid Salt Photocatalyst with High Photocatalytic Activity on Degradation of Dye

Chengsi Pan and Yongfa Zhu*

Department of Chemistry, Tsinghua University, Beijing, 100084, China

Tel: +86-10-62783586 Fax: +86-10-62787601 Email: zhuyf@mail.tsinghua.edu.cn

H$_2$O$_2$ Determination.[1] In hydrogen peroxide determination, 10ml sample taken from the reactor at given time intervals and 5ml of 0.1 mol/L potassium titanium (IV) oxalate solution were mixed and diluted to 25 ml. The absorbance of the mixture was measured at 400 nm using Hitachi U-3010 UV–vis spectrophotometer. 5ml of 0.1 mol/L potassium titanium (IV) oxalate solution were mixed 10ml MB. And then, the mixture was diluted to 25mL and used as the blank.

Table S1. Concentration of Hydrogen Peroxide during the Photocatalytic Reaction

Time (min)	0	5	10	15	20	25
H$_2$O$_2$ (mg/L)	0	0.11	0.52	1.07	1.70	2.74

1. Sellers, R. M. Spectrophotometric determination of hydrogen peroxide using potassium titanium (IV) oxalate. *Analyst* 1980, *150*, 950-954

Structure and Morphology. The products were characterized by characterized by powder X-ray diffraction (XRD) on Bruker D8-advance X-ray diffractometer at 40 kV and 40mA for monochromatizaed Cu K_α1 (λ =1.5406Å) radiation. The patterns were scanned from 10° to 70° (2θ) at a scanning rate of 10°/ min^{-1} with a step width of 0.02^o and time per step of 5.6s. Morphologies and structures of the prepared samples were further examined with JSM 6301 electron scanning microscope (SEM) and transmission electron microscopy (TEM) by a JEM 1010 electron microscope operated at an accelerating voltage of 100 kV. High-resolution TEM (HRTEM) images were obtained

with a JEM 2010F field emission gun transmission electron microscope operated at an accelerating voltage of 200 kV.
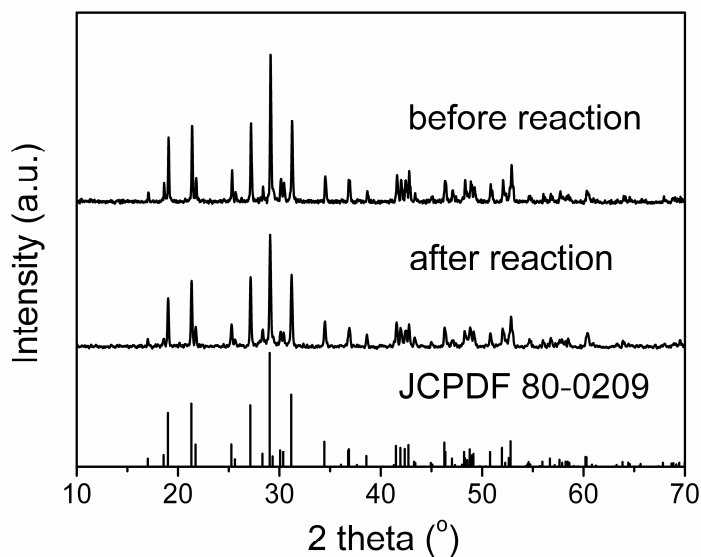

Figure S1. X-ray diffraction patterns of the $BiPO_4$. Before and after the reaction(one cycle).

The peak position is almost not changed after reaction. While the relative intensity becomes lower after reaction due to X-ray shielding caused by absorption of carbonaceous material during reaction. The intensity ratios of the reflections after reaction are a little higher. However, the change is all less than 5% error bar of XRD. The crystal size calculated from the peak (120) is 85.2nm before reaction and 85.0nm after reaction, which is below the error bar of XRD. Besides that, there are no new peaks in the XRD patterns after reaction. All the above discussion shows that the materials don't destruct after reaction.
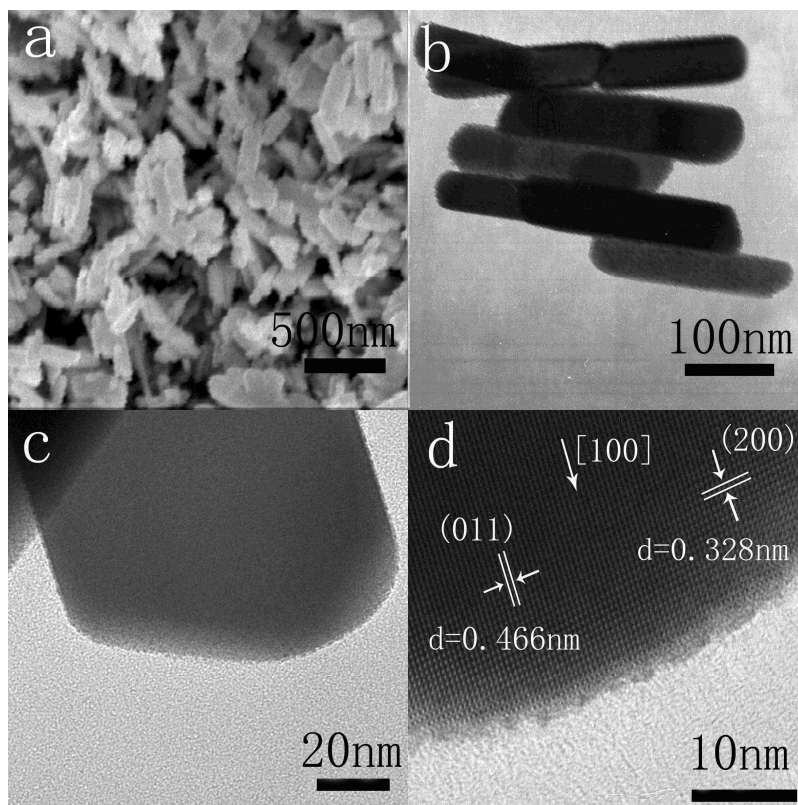
Figure S2. SEM(a), TEM(b) and HRTEM (c, d) images of BiPO$_4$ obtained from hydrothermal reaction.

Mott-Schottky Measurements. As-prepared samples for the fabrication of photo anode were obtained by mixing 1mL of ethanol and 20 mg of as-prepared powder homogeneously. The as-prepared samples were spread on the indium-tin oxide (ITO) conducting glass (3 cm×2 cm) with a sheet resistance of 30 Ω. After the films were dried under ambient conditions, they were sintered in air at 200 °C for 1 h. Mott-Schottky spectra were measured with a three electrode cell, using the BiPO$_4$ photo anode as a working electrode, a platinum wire as the counter electrode, and a standard Ag/AgCl in saturated KCl as the reference electrode. The electrolyte was 0.1M Na$_2$SO$_4$ (pH 7.2). Impedance spectra were obtained with a CHI660B equipped with an impedance analyzer and controlled by a computer.
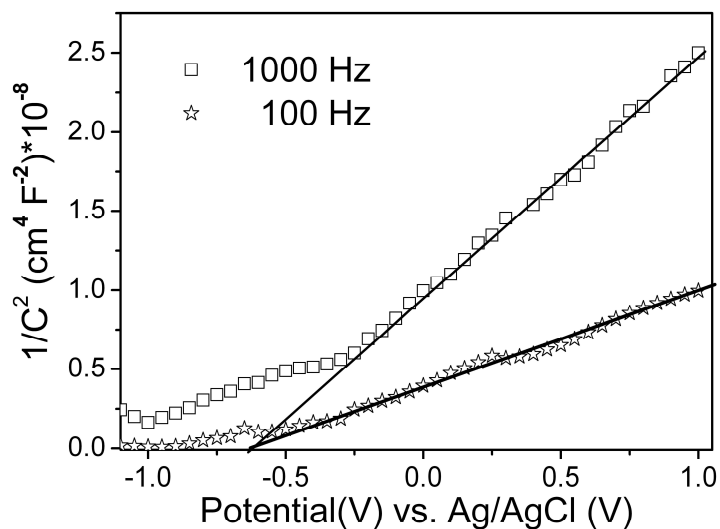
Figure S3. Mott-Schottky (MS) plots of the $BiPO_4$ catalyst film electrodes.

Photoelectrochemical measurements. The photoelectrochemical experiment was measured on an electrochemical system (CHI-660B, China). Photoelectrochemical measurements were carried out in a conventional three-electrode, single-compartment glass cell, fitted with a synthesized quartz window, using a potentiostat. The quartz electrolytic cell was filled with 0.1 M Na_2SO_4. The ITO/ $BiPO_4$ or ITO/TiO_2 electrodes served as the working electrode. The counter and the reference electrodes were platinum black wire and saturated calomel electrode (SCE), respectively. A 11 W germicidal lamp were used as the excitation light source for ultraviolet irradiation.
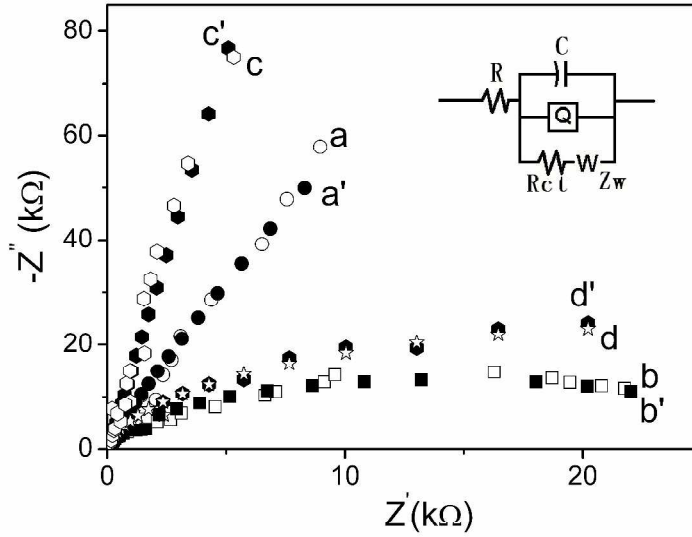
Figure S4. (A) Nyquist plots for BiPO$_4$ and P25 nanoparticle in aqueous solution under UV light illumination: (a, a') BiPO$_4$, dark, (b, b') BiPO$_4$, light on, and (c, c') P25, dark (d, d') P25, light on. Hollow symbols (a, b, c, d) and dark dots (a', b', c', d') indicate the experimental data and fitted curves, respectively. Inset is the equivalent electric circuit of the electrochemical system. R: bulk electrolyte resistance. Q: electrochemical double-layer capacitance. C: space charge capacitance. Rct: charge-transfer resistance. Zw: Warburg impedance. The constant phase element (CPE) Q can replace the electrochemical double-layer capacitance at the electrode-electrolyte interface. The impedance of CPE is given as follows $Q = \dfrac{1}{Y(j\omega)^n}$, where Y is the admittance magnitude of CPE and n is the exponent related to the phase angle $\varphi = n\,(\pi/2)$.

Table S2 Parameters Extracted from Fitted Results of EIS Spectra for BiPO$_4$ and P25

	R(Ω)	C (μF)	Q (Ssec^n)	n	R$_{ct}$ (kΩ)	Z (Ssec$^{0.5}$)
BiPO$_4$ (Dark)	48.09	32.68	$2.715*10^{-5}$	0.8574	204.8	8.706×10^{-5}
BiPO$_4$ (UV)	47.99	36.93	$2.331*10^{-5}$	0.8563	28.82	9.067×10^{-4}
P25 (Dark)	48.09	43.35	$2.311*10^{-5}$	0.8790	243.2	8.152×10^{-5}
P25 (UV)	47.99	58.12	$2.097*10^{-5}$	0.8573	48.82	8.065×10^{-4}

Band Structure Calculation

Electronic structure of $BiPO_4$ was calculated by the CASTEP program, based on density functional theory (DFT). The plane-wave pseudopotential method was used to optimize crystal geometries, to obtain the corresponding electronic band structures. In these calculations, the energy cutoff was chosen at 380 eV. The generalized gradient approximation (GGA) with Perdew, Burke and Ernzerhof (PBE) exchange correlation functional was adopted. Ultrasoft pseudopotentials were used for bismuth, phosphor, and oxygen atoms. The Brillouin-zone sampling was performed by using a k-grid of $4 \times 4 \times 4$ points for the calculations. The respective high-symmetry points are G (0, 0, 0), Z (0, 0, 1/2), Y (0, 1/2, 0), A (-1/2, 1/2, 0), B(-1/2, 0, 0), D(-1/2, 0, 1/2), E(-1/2, 1/2, 1/2), C(0, 1/2, 1/2), and in terms of the reciprocal basis vectors.
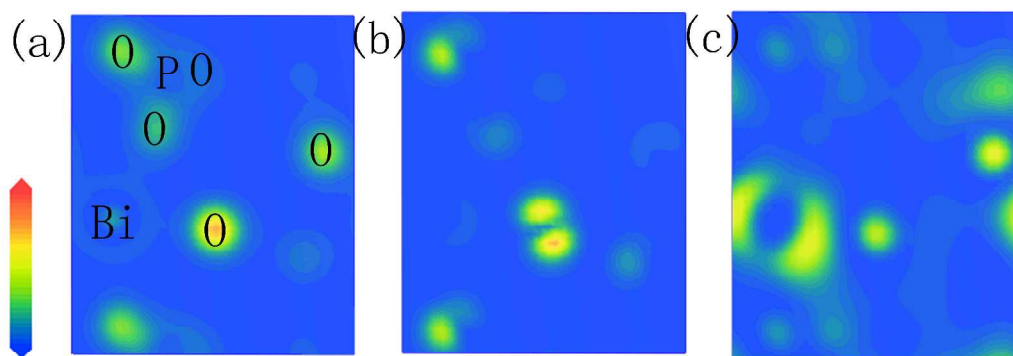

Figure S5. Charge density contour plots through a plane parallelled to (001) containing both Bi and P atoms: (a) total electron density, (Plotted from 0 (blue) to red 7.00 (red) $e \cdot Å^{-3}$.), (b) HOMO, and (c) LUMO. (Plotted from 0 (blue) to red 0.05 (red) $e \cdot Å^{-3}$)